Molecular Crystals and Liquid Crystals
Publication details, including instructions for authors and subscription information:
http://www.tandfonline.com/loi/gmcl20

# Spontaneous Polarization in Smectic A Phase of Carbon Nanotubes Doped Deformed Helix Ferroelectric Liquid Crystal

Jai Prakash [a], Ajay Kumar [b], Tilak Joshi [b], Dalip S. Mehta [a], Ashok M. Biradar [b] & W. Haase [c]

[a] Instrument Design Development Centre, Indian Institute of Technology Delhi, Hauz Khas, New Delhi, India

[b] Liquid Crystal Group, National Physical Laboratory, Dr. K. S. Krishnan Road, New Delhi, India

[c] Institute of Physical Chemistry, Technical University Darmstadt, Darmstadt, Germany

Version of record first published: 30 Jun 2011

To cite this article: Jai Prakash, Ajay Kumar, Tilak Joshi, Dalip S. Mehta, Ashok M. Biradar & W. Haase (2011): Spontaneous Polarization in Smectic A Phase of Carbon Nanotubes Doped Deformed Helix Ferroelectric Liquid Crystal, Molecular Crystals and Liquid Crystals, 541:1, 166/[404]-176/[414]

To link to this article: http://dx.doi.org/10.1080/15421406.2011.570216

*Mol. Cryst. Liq. Cryst.*, Vol. 541: pp. 166/[404]–176/[414], 2011

ISSN: 1542-1406 print/1563-5287 online
DOI: 10.1080/15421406.2011.570216



# Spontaneous Polarization in Smectic A Phase of Carbon Nanotubes Doped Deformed Helix Ferroelectric Liquid Crystal

JAI PRAKASH,[1] AJAY KUMAR,[2] TILAK JOSHI,[2] DALIP S. MEHTA,[1] ASHOK M. BIRADAR,[2] AND W. HAASE[3]

[1]Instrument Design Development Centre, Indian Institute of Technology Delhi, Hauz Khas, New Delhi, India
[2]Liquid Crystal Group, National Physical Laboratory, Dr. K. S. Krishnan Road, New Delhi, India
[3]Institute of Physical Chemistry, Technical University Darmstadt, Darmstadt, Germany

*Observation of non-zero spontaneous polarization in paraelectric phase in multiwalled carbon nanotubes doped deformed helix ferroelectric LC is reported. Electro-optical response, spontaneous polarization, rotational viscosity, dielectric permittivity, dielectric loss factor, and electrical resistance of pure and multiwalled carbon nanotubes doped deformed helix ferroelectric LC have been measured. Non-zero spontaneous polarization in paraelectric phase has been attributed to the possible short range orientational order of deformed helix ferroelectric LC surrounding the multiwalled carbon nanotubes through surface anchoring and ionic impurities. The results presented will help to understand the basic mechanism of interaction of multiwalled carbon nanotubes with deformed helix ferroelectric LC.*

**Keywords** Carbon nanotubes; deformed helix ferroelectric liquid crystal; dielectric properties; rotational viscosity; spontaneous polarization

## 1. Introduction

Carbon nanotubes (CNTs) have drawn a great deal of attention in fundamental and applied research since their discovery by Iijima in 1991 [1]. Various important devices such as field-effect transistors, memory storage devices, sensors and actuators, and field emission sources have been employed using CNTs due to their fascinating electrical, dielectric, thermal, mechanical, and electronic properties [2–6]. The doping of CNTs in liquid crystals (LCs) has been pursued by various groups for improving their electro-optical properties, dynamic response, and other physical parameters [7–13]. However, much of the reported work based on CNTs/LC dispersions has

Address correspondence to Ashok M. Biradar, Liquid Crystal Group, National Physical Laboratory, Dr. K. S. Krishnan Road, New Delhi-110012, India. E-mail: abiradar@mail.nplindia.ernet.in

been focused on nematic liquid crystals (NLCs) [8–10,13]. The doping of CNTs in ferroelectric liquid crystals (FLCs) is rarely reported in literature. However, few studies based on CNTs/FLCs dispersions have been presented recently by different research groups [14–17]. Lagerwall *et al.* have studied the effect of single walled CNTs (SWCNTs) on antiferroelectric LCs by adding CNTs indirectly employing a NLC and observed the changes in the phase sequences of the material [14]. The electro-optical studies based on FLCs/SWCNTs dispersion have revealed the fastening of switching response due to the trapping of ions by SWCNTs [15,16]. The deformed helix FLCs (DHFLCs) have much applications in display devices because of their low driving voltage, gray scale generation capability, easily achievable alignment (even in thicker cells), fast response, etc. [18,19]. The effect of MWCNTs on the electro-optical response of DHFLC material (FLC 6304) at room temperature has been demonstrated by our group recently [20]. The fastening of response in CNTs doped DHFLC material has been observed and attributed to decrease in rotational viscosity and increase in anchoring energy.

In this article, we report the effect of MWCNTs on the behavior of spontaneous polarization ($P_S$) of DHFLC material, namely LAHS 18, with temperature. The material LAHS 18 is a newly synthesized DHFLC. The molecular compositions and characterization of this material has been presented elsewhere [21]. We observed that the value of $P_S$ of MWCNTs doped LAHS 18 do not vanish at SmC*-SmA* transition temperature ($T_C$) and showed some remarkable contribution even in SmA* and isotropic phases. The occurrence of this non zero $P_S$ in SmA* phase has been analyzed by electro-optical, dielectric relaxation and resistance measurements. It was attributed to short range orientational ordering of DHFLC molecules around MWCNTs and ionic impurities present in the mixture.

## 2. Experimental

The MWCNTs were synthesized by chemical vapor deposition method. The diameter of synthesized MWCNTs ranged 30–50 nm with typical length ranging from 0.3 μm to several μm. A small amount (~0.1 wt%) of MWCNTs was doped into LAHS 18 and the mixture was ultrasonicated for 3 h to reduce the agglomeration tendency of CNTs. The sample cells for the present study were prepared using indium tin oxide (ITO) coated glass plates. The desired (squared) pattern area was $0.45 \times 0.45\,cm^2$. The thickness of the cell was maintained by using 4 μm thick Mylar spacers. The material (pure and MWCNTs doped LAHS 18) was filled into these cells by capillary action above isotropic temperature. For homogeneous alignment of the FLC cells, spin coating of polyimide (nylon 6/6) followed by smooth rubbing of the substrate has been carried out using buffing machine. The phase sequence of DHFLC material used is as follows:

$$Cr. \overset{1^\circ C}{\longleftrightarrow} SmC^* \overset{57.5^\circ C}{\longleftrightarrow} SmA^* \overset{64^\circ C}{\longleftrightarrow} I. \qquad \text{(LAHS18)}$$

The various material parameters such as $P_S$ and rotational viscosity ($\eta$) of pure and MWCNTs doped LAHS 18 material have been determined using automatic LC tester (ALCT-P, Instec, USA). For electrical response of the sample, the triangular wave pulse (20 $V_{PP}$) generated from the function generator was applied to the sample and studied by using a storage oscilloscope (HM 1507–3, HAMEG, Germany)

interfaced with the computer via SP-107 software. The dielectric relaxation spectroscopy of pure and MWCNTs doped LAHS 18 material has been performed by using an impedance analyzer (Wayne Kerr, 6540A, UK) in the frequency range 20 Hz – 1 MHz with measuring voltage of 0.5 V.

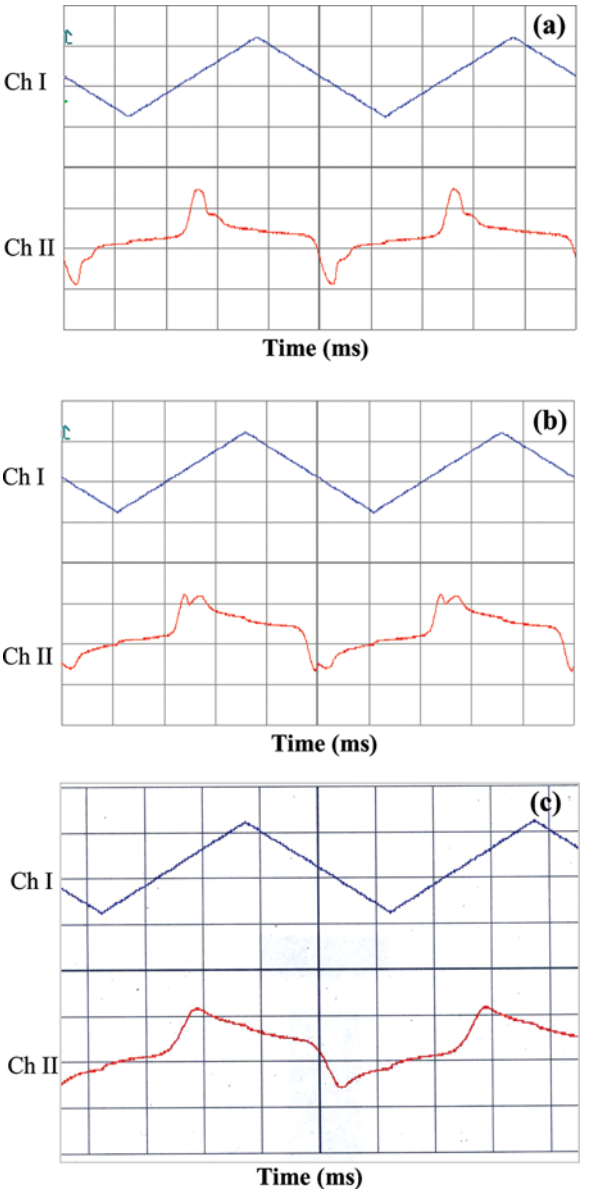


**Figure 1.** Electrical response of MWCNTs doped DHFLC (LAHS 18) at (a) 45°C, (b) 54°C and 58°C. Ch I shows driving triangular pulse voltage (20 $V_{PP}$) and Ch II shows its electrical response. The time scale per division is on *x*-axis, which is same for both channels. (Figure appears in color online.)

## 3. Results and Discussion

Figure 1 shows the electrical response of MWCNTs doped LAHS 18 sample cell on the application of triangular wave of amplitude 20 $V_{pp}$. In the output response, a single peak representing the coupling of molecular polarization with the applied electric field has been observed in deep $SmC^*$ phase. When the temperature is increased, a second peak of small amplitude along with the first peak has been observed

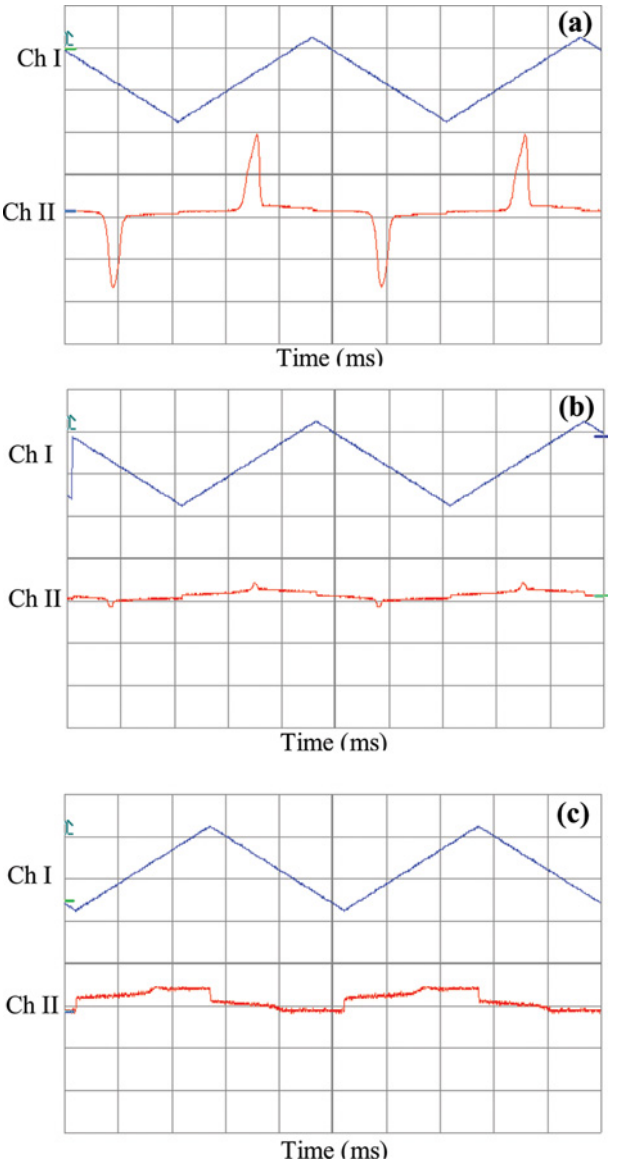


**Figure 2.** Electrical response of pure DHFLC (LAHS 18) at (a) 45°C, (b) 54°C and 58°C. Ch I shows driving triangular voltage (20 $V_{PP}$) and Ch II shows its electrical response. The time scale per division is on *x*-axis, which is same for both channels. (Figure appears in color online.)

(Fig. 1(a)). The amplitude of the second peak has increased as temperature approached to SmC*–SmA* phase transition temperature ($T_C$) and became comparable with that of first peak at $T_C$ (Fig. 1(b)). The first peak has been vanished completely at $T_C$ due to transition from ferroelectric to paraelectric ordering of the DHFLC molecules but, surprisingly, the second peak remained even in SmA* as well as in isotropic phase (Fig. 1(c)). Figure 2 show the electrical response of pure LAHS 18 on the application of triangular wave pulse of amplitude 20 $V_{PP}$. It is clearly reflected from figure that only a single polarization peak has been appeared which almost disappeared in SmA*. The contribution of second peak to $P_S$ in MWCNTs doped LAHS 18 has been analyzed by observing the behaviors of $P_S$ and $\eta$ with temperature. Figure 3 shows the behavior of $P_S$ and $\eta$ with temperature in pure and MWCNTs doped LAHS 18. From Figure 3(a), it can be seen that the value of $P_S$

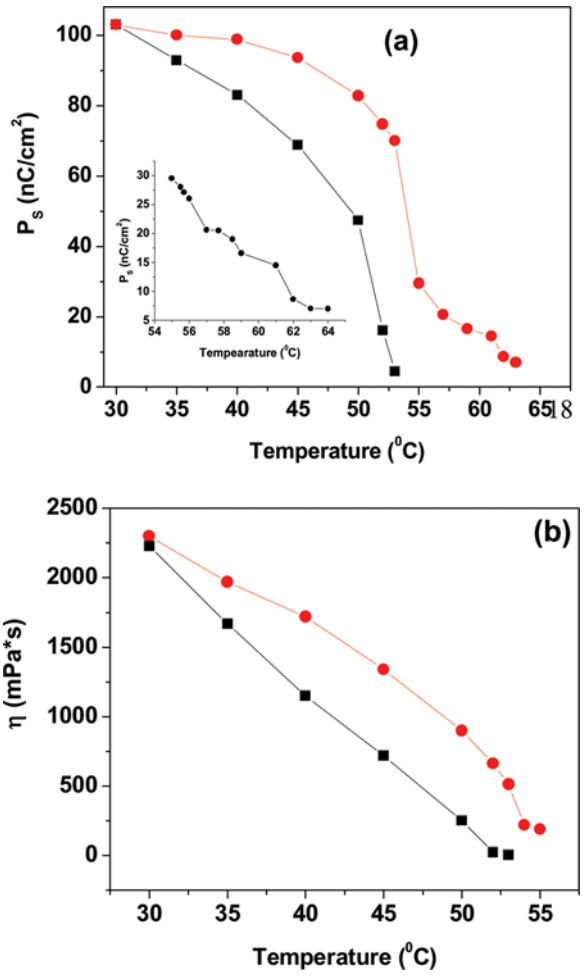


**Figure 3.** Behavior of (a) spontaneous polarization ($P_S$) and (b) rotational viscosity ($\eta$) of pure (squares) and MWCNTs doped (circles) LAHS 18 with temperature. The inset of (a) shows the behavior of $P_S$ of MWCNTs doped LAHS 18 material close to $T_C$. (Figure appears in color online.)

decreases gradually for MWCNTs doped LAHS 18 whereas it shows rapid decrease in case of pure LAHS 18. Also, $P_S$ remains higher for MWCNTs doped LAHS 18 than that of pure LAHS 18 on increasing the temperature. The difference in the $P_S$ values of MWCNTs doped and pure LAHS 18 is found to be more significant near $T_C$ (inset of Fig. 2(a)). The retention of higher values of $P_S$ suggested the increase in the strength of $SmC^*$ phase by dispersing MWCNTs into the LAHS 18 material. Lagerwall *et al.* observed the increase in the strength of $SmC^*$ phase of CNTs doped Anti-FLCs and demonstrated the possibility of increase in $P_S$ or a longer helical pitch [22]. The behavior of $\eta$ of MWCNTs doped LAHS 18 with temperature exhibited the same trend as $P_S$. There is a substantial change in pure and MWCNTs doped LAHS 18 which is clearly reflected from Figure 3(b).

We have also performed the dielectric measurements on pure and MWCNTs doped LAHS 18 with temperature. Figure 4 exhibits the behavior of real part of dielectric permittivity ($\varepsilon'$) of MWCNTs doped and pure LAHS 18 at temperatures (from below $T_C$ to isotropic phase). It is quite obvious from Figure 4 that value of dielectric strength ($\Delta\varepsilon = \varepsilon_0 - \varepsilon_\infty$) of MWCNTs doped LAHS 18 is greater than that of pure LAHS 18 as the value of $\varepsilon'$ is slightly higher for MWCNTs doped LAHS 18 than that of pure LAHS 18 in the low frequency regime. It has been observed that the incorporation of CNTs in the LCs shifted the $T_C$ of mixture to higher values.

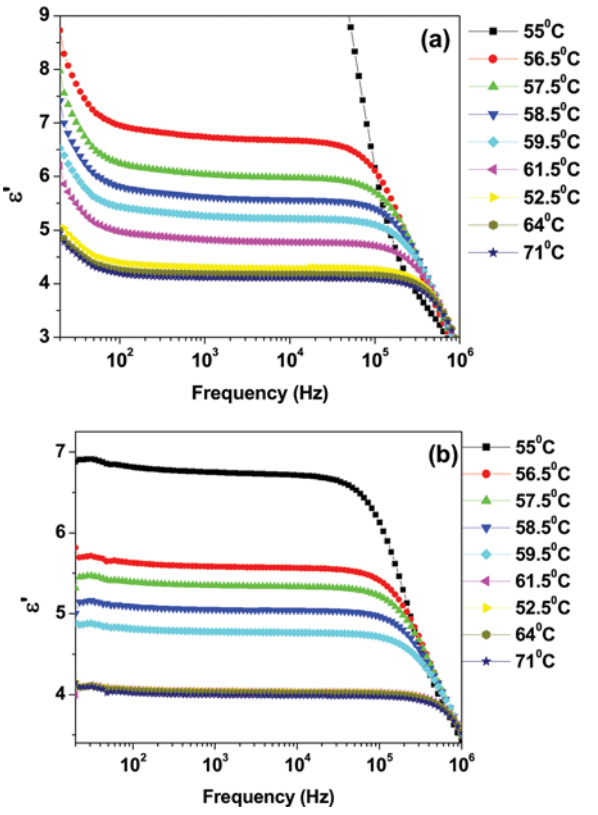


**Figure 4.** Behavior of real part of dielectric permittivity ($\varepsilon'$) of (a) MWCNTs doped LAHS 18 and (b) pure LAHS 18 material with frequency in $SmA^*$ and isotropic phase.

Duran *et al.* have studied the effect of CNTs on the nematic-isotropic phase transition temperature ($T_{NI}$) and found that $T_{NI}$ was enhanced for a certain range of concentration of CNTs [23]. We have also observed the same effect in MWCNTs doped LAHS 18 material. However, the shift in $T_C$ in our case is very less (~1°C). Figure 5 shows the behavior of dielectric loss factor (tan $\delta$) of MWCNTs doped and pure LAHS 18 with temperature. Usually by using impedance analyzers one measures capacitance and tan $\delta$ of the sample, where tan $\delta$ is defined as the ratio of imaginary and real part of the dielectric permittivity [24]. The value of tan $\delta$ for MWCNTs doped LAHS 18 is found to be almost one order higher than that of pure LAHS 18 at low frequencies (Figs. 5(a) and 5(b)). This increase in tan $\delta$ is due to the increase in electrical conductivity of LAHS 18 by MWCNTs [25]. Lebovko *et al.* have also observed the sharp increase in the electrical conductivity of CNTs doped LC due to the formation of continuous network of CNTs in LC matrix [26]. Figure 6 shows the behavior of resistance of pure and MWCNTs doped DHFLC (LAHS 18) with frequency. It can be seen clearly from Figure 6(a) that the electrical resistance

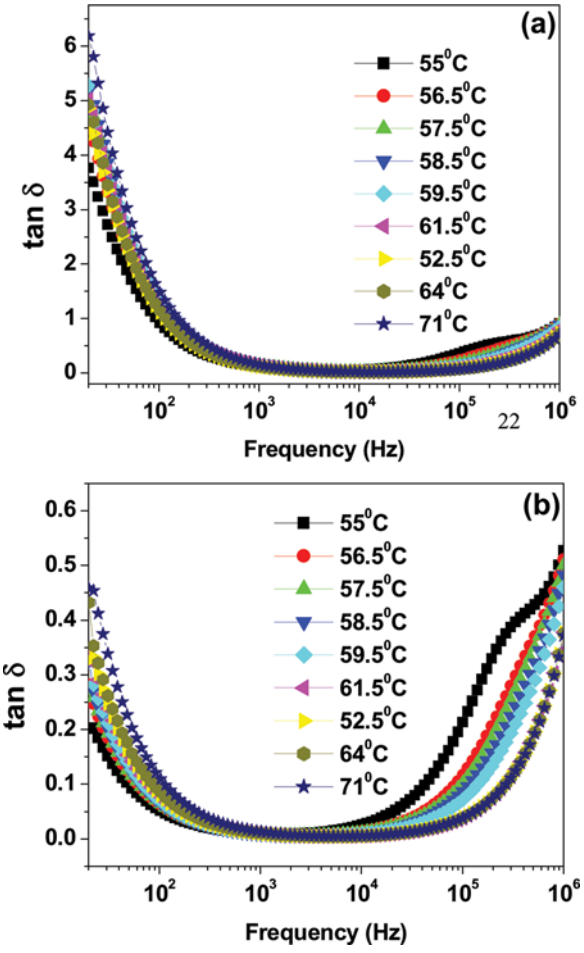


**Figure 5.** Behavior of dielectric loss factor (tan $\delta$) of (a) MWCNTs doped LAHS 18 and (b) pure LAHS 18 material with frequency in SmA* and isotropic phase.

of MWCNTs doped LAHS 18 is almost one order lower than that of pure LAHS 18 (Fig. 6(b)). The lower values of electrical resistance inferred the increased conductivity of MWCNTs doped LAHS 18 material. We have also performed the measurements to observe the effect of MWCNTs on dielectric memory of LAHS 18 material with temperature. Figure 7(a) shows the variation of $\varepsilon'$ on the application of dc biases of 0 V, 8 V and 0 V again at room temperature. In the absence of any dc bias across cell (0 V state) the value of $\varepsilon'$ comes out to be high due to the Goldstone mode (GM) contribution. This GM contribution gets suppressed on the application of certain dc bias and result in lower values of $\varepsilon'$. If the value of $\varepsilon'$ attains its original value (0 V state) on the removal of bias then it means material does not possess dielectric memory. On the other hand, the retention of $\varepsilon'$ values in switched state even after removal of bias indicates the dielectric memory. Figure 7(a) shows the behavior of dielectric memory of MWCNTs doped LAHS 18 at room temperature. It is clear from figure that the CNTs doped material does not show memory at room temperature. The dielectric memory of MWCNTs doped LAHS 18 material has been enhanced on increasing the temperature and become more significant close to Tc.



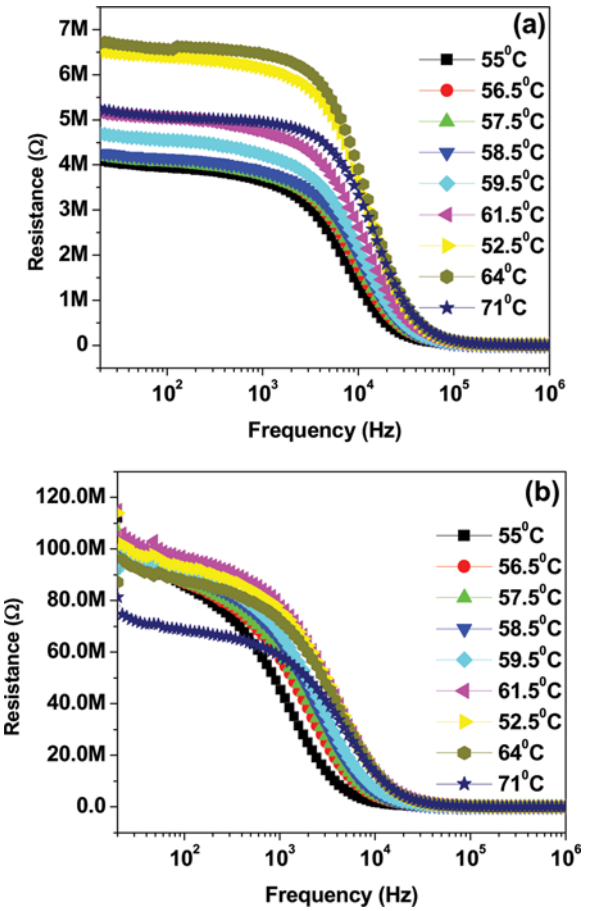


**Figure 6.** Behavior of electrical resistance of (a) MWCNTs doped LAHS 18 and (b) pure LAHS 18 material with frequency in SmA* and isotropic phase.

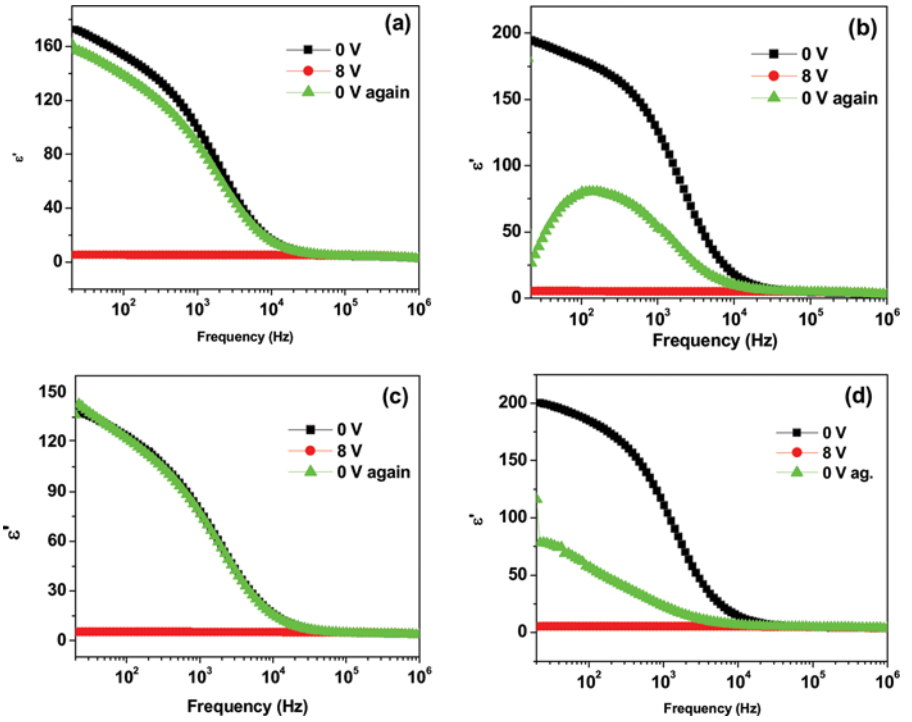


**Figure 7.** Behavior of dielectric memory of (a), (b) MWCNTs doped LAHS 18 and (c), (d) pure LAHS 18 material with temperature.

Figure 7(b) reflects the occurrence of remarkable memory effect at 52.4°C which is very close to Tc. The pure LAHS 18 material also shows the same behavior as MWCNTs doped LAHS 18 with temperature that can be seen from Figs. 7(c) and 7(d). But, the behavior of $\varepsilon'$ of memory state (0 V again) has been found to show remarkable change in case of MWCNTs doped LAHS 18. The behavior of memory state (0 V again curve) is somewhat different in MWCNTs doped LAHS 18 unlike pure one at low frequency regime (Fig. 7(d)). The long axis of CNTs orients parallel to the LC director with an orientational order parameter (S) between 0.6 and 0.9 which is higher than that of pure LC [27–29]. Baik *et al.* demonstrated the strong interaction between LC-CNT to be a consequence of surface anchoring of LC molecules on CNTs with a binding energy of $-2$ eV for $\pi$-$\pi$ stacking [30]. The coupling of LC molecules with CNTs through surface anchoring can induce local short range orientational order of LC molecules surrounding the CNTs. Basu *et al.* have demonstrated that this short range orientational order generates so called ''Pseudo-nematic domains'' having polarization and hence respond to applied electric field [31]. The occurrence of the second peak may be attributed to the coupling between polarizations of DHFLC molecules anchored on CNT surfaces and applied electric field. When the temperature increases, the value of $P_S$ decreases and hence the coupling between electric field and $P_S$ of those molecules surrounding MWCNTs become enough significant to appear as a second polarization peak in the output. At temperatures just above $T_C$, the polarization of DHFLC molecules (except those surrounding MWCNTs) has been vanished. The molecules surrounding MWCNTs

surfaces retain some ordering such that they possess non-zero polarization which on coupling with electric field produce second peak. However, the behaviors of $\tan\delta$, electrical resistance, and dielectric memory with temperature at low frequency regime suggest the intense signature of ionic impurities in MWCNTs doped DHFLC. The low frequency increase in $\varepsilon'$ and $\tan\delta$ are classic signatures of ions, their slow motion through the sample may give polarization processes longer relaxation times. The lower value of electrical resistance in case of MWCNTs doped LAHS 18 suggested that all MWCNTs have not aligned along the director. Few of them have formed aggregates and their short circuiting has given lower values of resistance. The presence of ions gave rise to low relaxation processes that can go from seconds or even minutes after removal of bias. This phenomenon has been appeared clearly from the low frequency dielectric memory near $T_C$. Thus, ionic contaminations may also result second polarization peak (which also appeared in isotropic phase) in the electrical response of MWCNTs doped LAHS 18 material.



## 4. Conclusions

A finite value of $P_S$ in $SmA^*$ phase of MWCNTs doped LAHS 18 has been observed. The occurrence of $P_S$ has been confirmed by means of electro-optical and dielectric methods. It is found that the non-zero $P_S$ in $SmA^*$ may arise due to MWCNTs induced short range ordering of DHFLC molecules as well as the introduction of ionic impurities in DHFLC material while doping with MWCNTs. However, the experimental results have been found favorable to the contribution of excess ionic contaminations to produce non-zero $P_S$ in $SmA^*$ phase of MWCNTs doped LAHS 18 material.

## References

[1] Iijima, S. (1991). *Nature (London)*, *354*, 56.
[2] Martel, R., Schmidt, T., Shea, H. R., Hertel, T., & Avouris, Ph. (1998). *Appl. Phys. Lett.*, *73*, 2447.
[3] Rueckes, T., Kim, K., Joselevich, E., Tseng, G. Y., Cheung, C. L., & Lieber, C. M. (2000). *Science*, *289*, 94.
[4] Kong, J., Franklin, N. R., Zhou, C., Chapline, M. G., Peng, S., Cho, K., & Dai, H. (2000). *Science*, *287*, 622.
[5] Rajmani, X. Yu, R., Stelson, K. A., & Cui, T. (2006). *Sens. Actuators*, *A 132*, 626.
[6] Baughman, R. H., Zakhidov, A. A., & de Heer, W. A. (2002). *Science*, *297*, 787.
[7] Lee, W., Wang, C. Y., & Shih, Y. C. (2004). *Appl. Phys. Lett.*, *85*, 513.
[8] Chen, H. Y., Lee, W., & Clark, N. A. (2007). *Appl. Phys. Lett.*, *90*, 033510.
[9] Jeon, S. Y., Shin, S. H., Jeong, S. J., Lee, S. H., Jeong, S. H., Lee, Y. H., Choi, H. C., & Kim, K. J. (2007). *Appl. Phys. Lett.*, *90*, 121901.
[10] Lu, S. Y., & Chien, L. C. (2008). *Opt. Exp.*, *16*, 12777.
[11] Jeon, S. Y., Park, K. A., Baik, I. S., Jeong, S. J., Jeong, S. H., An, K. H., Lee, S. H., & Lee, Y. H. (2007). *NANO*, *2*, 41.
[12] Baik, I. S., Jeon, S. Y., Lee, S. H., Park, K. A., Jeong, S. H., An, K. H., & Lee, Y. H. (2005). *Appl. Phys. Lett.*, *87*, 263110.
[13] Chen, H. Y., & Lee, W. (2006). *Appl. Phys. Lett.*, *88*, 222105.
[14] Lagerwall, J. P. F., Dabrowski, R., & Scalia, G. (2007). *J. Non-Cryst. Solids*, *353*, 441.
[15] Arora, P., Mikulko, A., Podgornov, F., & Haase, W. (2009). *Mol. Cryst. Liq. Cryst.*, *502*, 1.

[16] Podgornov, F., Suvorova, A., Lapanik, A., & Haase, W. (2009). *Chem. Phys. Lett.*, *479*, 206.
[17] Malik, P., Choudhary, A., & Raina, K. K. (2009). *Asian J. Chem.*, *21*, S095.
[18] Beresnev, L. A., Chigrinov, V. G., Dergachev, D. I., Poshidaev, E. P., Funfschilling, J., & Schadt, M. (1989). *Liq. Cryst.*, *5*, 1171.
[19] Funfschilling, J., & Schadt, M. (1989). *J. Appl. Phys.*, *66*, 3877.
[20] Prakash, J., Choudhary, A., Mehta, D. S., & Biradar, A. M. (2009). *Phys. Rev. E*, *80*, 012701.
[21] Kumar, A., Prakash, J., Biradar, A. M., & Haase, W. (2010). *Appl. Phys. Exp.*, *3*, 091701.
[22] Lagerwall, J. P. F., Dabrowski, R., & Scalia, G. (2007). *J. Non-Cryst. Solids*, *353*, 4411.
[23] Duran, H., Gazdecki, B., Yamashita, A., & Kyu, T. (2005). *Liq. Cryst.*, *32*, 815.
[24] Haase, W., & Wrobel, S. (2003). *Relaxation Phenomena: Liquid Crystals, Magnetic Systems, Polymers, High-Tc Superconductors, Metallic Glasses*, Springer-Verlag: Berlin Heidelberg, 18.
[25] Lu, S.-Y., & Chien, L.-C. (2008). *Opt. Exp.*, *16*, 12777.
[26] Lebovka, N., Dadakova, T., Lysetskiy, L., Melezhyk, O., Puchkovska, G., Gavrilko, T., Baran, J., & Drozd, M. *J. Mol. Struct.* Accepted.
[27] Lynch, M. D., & Patrick, D. L. (2002). *Nano Lett.*, *2*, 1197.
[28] Dierking, I., Scalia, G., & Morales, P. (2005). *J. Appl. Phys.*, *97*, 044309.
[29] Scalia, G., Lagerwall, J. P. F., Schymura, S., Haluska, M., Giesselmann, F., & Roth, S. (2007). *Phys. Stat. Sol.* (b), 244.
[30] Baik, I. S., Jeon, S. Y., Lee, S. H., Park, K. A., Jeong, S. H., An, K. H., & Lee, Y. H. (2005). *Appl. Phys. Lett.*, *87*, 263110.
[31] Basu, R., & Iannacchione, G. S. (2009). *Appl. Phys. Lett.*, *95*, 173113.